Available online at www.sciencedirect.com

ScienceDirect

IFAC PapersOnLine 51-9 (2018) 329–336

Feedback Traffic Control at Highway Work Zones using Variable Speed Limits

Ioannis Papamichail*, Markos Papageorgiou*, Ioannis Stamatakis**

**Dynamic Systems and Simulation Laboratory, Technical University of Crete, 73100 Chania, Greece (Tel: +30 2821037422; e-mail: <ipapa, markos> @dssl.tuc.gr)*

***SCHLOTHAUER & WAUER GmbH, Richard-Reitzner-Allee 1, 85540 Haar, Germany (Tel: +49 8921187805; e-mail: i.stamatakis@schlothauer.de*

Abstract: This paper presents a novel real-time merging traffic control approach for throughput maximization at highway work zones using Variable Speed Limits (VSL). A Proportional-Integral (PI) feedback regulator is employed for control which is simpler and potentially more robust compared to heuristic or optimal control procedures. Practical VSL implementation aspects have been taken into account. The proposed concept is demonstrated and evaluated using a validated microscopic traffic flow model for a real motorway work zone in Germany. Remarkable improvements can be observed for all performance indexes considered and for all replications simulated. Investigations have been carried out for different compliance rates, different set points utilized by the feedback regulator, as well as for different values of the lower admissible bound of the VSL. The proposed approach is deemed suitable for field implementation.

Keywords: work zone; variable speed limits; traffic control

1. INTRODUCTION

Work zone management aims at safe working conditions for work-zone workers, as well as safe and efficient passage of vehicles. An extensive report by the FHWA (2005) provides very useful insights on motivation, traffic management possibilities and impact. This paper addresses the sub-class of major highway work zones, where one or more lanes need to be closed over a period of several days or months; as a consequence, the traffic flow approaching the work zone needs to merge into a lower number of lanes within a limited space. When the arriving flow reaches or exceeds the reduced downstream capacity, congestion is created, leading to an additional, congestion-induced capacity drop. Although the exact reasons for the occurrence of capacity drop have not been fully explored until now, a major influencing factor is deemed to be due to the need for vehicles to accelerate from low speeds within the congestion to higher speeds downstream of the congestion head (Papageorgiou et al., 2008; Yuan et al., 2015; Yuan et al., 2016).

Several strategies have been proposed or used to ameliorate traffic conditions at work zones, some of which are reviewed here below:

- Variable Speed Limit (VSL) control algorithms for throughput maximization at highway work zones were proposed and tested via microscopic simulation by Lin et al. (2004) and Kang et al. (2004). Up to that point, most of the VSL studies for highway operations had focused mainly on safety-related issues.
- Microscopic simulation studies were also conducted for lane-based signal systems for merge control at work zones (Wei and Pavithran, 2006; Yang et al., 2009; Kang and Chang, 2009).
- A field evaluation of an advisory VSL system indicated a reduction of the average maximum speed difference along the work zone area and an increase of the total throughput (Kwon et al., 2015).
- Real-time merging traffic control aiming at throughput maximization at work zones in a similar way as the mainstream traffic flow control concept (Carlson et al., 2010), albeit by use of traffic lights instead of VSL, was proposed and tested via microscopic simulation by Papageorgiou et al. (2008) and Lentzakis et al. (2008).
- A microscopic simulation model was also used to evaluate a threshold-based VSL system by Fudala and Fontaine (2010). The onset of congestion was delayed, provided that demand volumes were not too far above the work zone capacity. Another conclusion was that signs must be positioned so that drivers accelerate back to a reasonable speed as they pass through a bottleneck.
- A simulation-based evaluation demonstrated that an integrated system (Kang and Chang, 2011) of a previously proposed VSL strategy (Lin et al., 2004; Kang et al., 2004) and a lane-based signal system (Kang and Chang, 2009) was yielding higher throughput compared to the lane-based signal system without VSL.
- Two simplified dynamic lane merging systems were compared using data collected from a real work zone (Harb et al., 2011).
- Recently, an optimal VSL control system, cast in a rolling horizon mode, for freeway work zone operations was presented and tested using a microscopic simulation model, showing promising results for the operational efficiency of the system (Yang et al., 2017).

2405-8963 © 2018, IFAC (International Federation of Automatic Control) Hosting by Elsevier Ltd. All rights reserved.
Peer review under responsibility of International Federation of Automatic Control.
10.1016/j.ifacol.2018.07.054

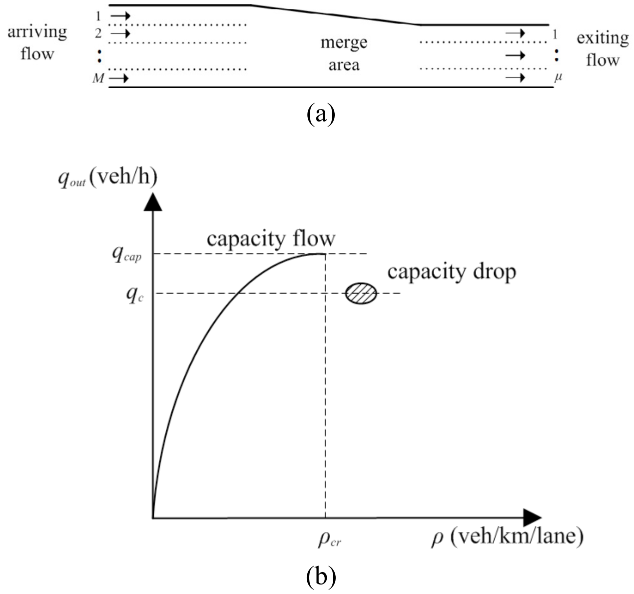

Fig. 1. (a) A typical work zone merge infrastructure; (b) The fundamental diagram at a highway work zone with lane drop.

This paper is based on previous work (Papageorgiou et al., 2008; Lentzakis et al., 2008; Tympakianaki et al., 2014), but uses VSL, instead of traffic lights, as a control actuator for efficient real-time merging traffic control at highway work zones. In contrast to other mentioned VSL-based approaches, a classical Proportional-Integral (PI) feedback regulator is employed for VSL work zone control, which is simpler and potentially more robust compared to heuristic or optimal control procedures. The proposed concept is tested using a validated microscopic traffic flow model for a real motorway work zone in Germany.

2. REAL-TIME MERGING TRAFFIC CONTROL FRAMEWORK

The proposed real-time merging traffic control framework follows the structure discussed in previous work (Papageorgiou et al., 2008; Lentzakis et al., 2008). Some main elements of that approach are presented here, along with the details of the novel VSL control for work zones.

2.1 Merge Area

Fig. 1(a) sketches a typical work zone merge infrastructure. The vehicles arriving on M lanes must change lanes appropriately so as to fit to the μ lanes ($\mu < M$) of the exit. The capacity at the exit of the merge area is lower than the upstream highway capacity due to the drop of one or more lanes. A typical flow-density diagram for the work zone infrastructure is presented in Fig. 1(b), where q_{out} is the traffic flow entering the narrower part of the infrastructure, and ρ is the density at the bottleneck location. When the arriving flow from upstream, and hence the bottleneck density, are small, merging conflicts are scarce and swift, and the exit flow q_{out} is correspondingly low. As the arriving flow, and hence ρ, increase, merging conflicts may increase, but q_{out} increases as well until, for a specific critical value ρ_{cr}, the exit flow reaches the downstream capacity q_{cap}. If ρ increases beyond ρ_{cr}, merging conflicts become more serious, leading to substantial vehicle decelerations and eventual accelerations that reduce the exit flow to lower values q_{c}, where $q_{\text{cap}} - q_{\text{c}}$ is the capacity drop due to congestion, which is deemed to depend on vehicle acceleration at the congestion head (Yuan et al., 2015; Yuan et al., 2016). Under these conditions, real-time control of the arriving flow may be employed in order to hold back traffic and maintain the density ρ at the bottleneck close to its critical value ρ_{cr}, and eventually maintain maximum throughput.

2.2 Control Devices and Real-Time Measurements

Holding back of arriving traffic may be materialized by use of different control devices. A control device that has been applied in previous work (Papageorgiou et al., 2008; Lentzakis et al., 2008; Tympakianaki et al., 2014) to regulate the arriving flow at the work zone area is a set of traffic lights, one for each lane. Alternatively, VSL may be used for traffic flow control upstream of the work zone merge area, as in the case of mainstream traffic flow control (Carlson et al., 2010). The application of a low VSL at some stretch (application area) upstream of the work zone may lead to a controlled congestion. An acceleration area, downstream of the application area, ensures that vehicles have enough space to accelerate from low speeds in the VSL application area to the critical speed corresponding to capacity flow through the bottleneck. In addition, for safety reasons, VSL may also be applied upstream of the application area (safety area) so as to enable a gradual speed decrease for arriving vehicles; see Fig. 2.

In order to apply feedback control and maintain the bottleneck density ρ close to its critical value ρ_{cr}, real-time measurements or estimates of ρ are needed. A frequently practiced way of estimating ρ is by use of ordinary loop detectors measuring traffic occupancy, placed at appropriate positions (Vigos et al., 2008). Alternatively, one may directly employ occupancy measurements and target a critical occupancy value o_{cr} (instead of ρ_{cr}) as in ALINEA ramp metering (Papageorgiou et al., 1991).

2.3 Control Algorithm

Similarly to what was proposed in the past for the case of mainstream traffic flow control of ramp merging bottlenecks (Carlson et al., 2011; Carlson et al., 2013), a PI controller is used here for VSL-based work zone traffic control. The measured (or estimated) density $\rho(k)$ (or occupancy) at the bottleneck location at each discrete time instant k $(= 0,1,2,\ldots)$ is compared against the desired set-point $\hat{\rho}$. The set-point is typically selected around the critical density value, at which capacity flow is achieved at that location; and the aim of the feedback regulator is to keep the bottleneck density close to the selected set-point which guarantees maximum throughput. The PI-type regulator is given by:

$$vsl(k) = vsl(k-1) + K_I(\hat{\rho} - \rho(k)) + K_P(\rho(k-1) - \rho(k)) \qquad (1)$$

where $vsl(k)$ represents the output of the regulator at discrete time k, while K_I and K_P are the integral and

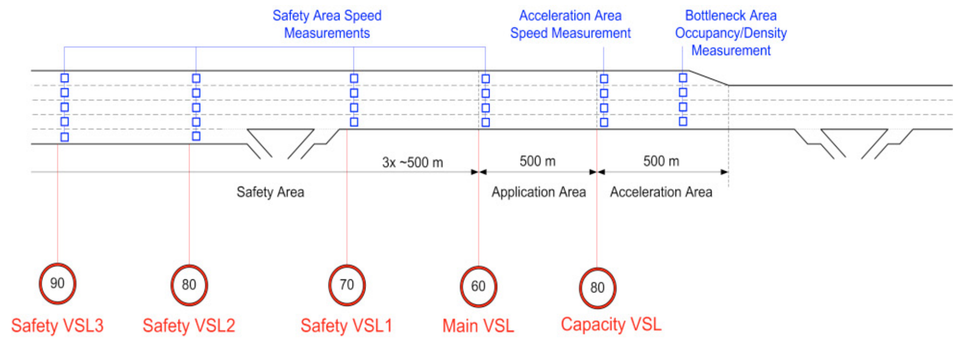

Fig. 2. Work zone and control infrastructure utilized.

proportional gains, respectively. The output of the regulator is truncated so as to remain within a range of admissible VSL values $[vsl_{\min}, vsl_{\max}]$. The truncated values are used at the next time-period as the $k-1$ values to avoid the well-known windup phenomenon for PI regulators.

Some practical VSL implementation aspects are then taken into account. Posted VSL can only take predefined discrete values (e.g. 90, 80, 70, … km/h). Furthermore, the difference between two consecutively posted VSL at the same gantry is limited (e.g. to $\pm 10\,\text{km/h}$), so as to avoid abrupt speed changes. Also, the difference between two VSL posted at consecutive gantries at the same control period is limited (e.g. to 10 km/h), as often required in practice, in order to achieve a safe approach of vehicles within the safety area. Finally, speed measurements from the area of each gantry may be used in order to ensure that the posted speed limit is not much higher than the measured speed.

3. APPLICATION SETUP

3.1 Road and Control Infrastructure Description

The described real-time VSL-based work zone traffic control framework is implemented, via microscopic simulation, at a motorway work zone infrastructure located on the A3 motorway in North Rhine-Westphalia (Germany), north-eastern of Cologne, in direction Leverkusen, between 133.71 and 132.82 km. The selected infrastructure features 4 arriving lanes and 3 exiting lanes, as depicted schematically in Fig. 2. Each lane has a width of 3.75 m. The total length of the simulated motorway stretch is about 3.5 km to accommodate any forming queue length. It also includes 2 couples of off-/on-ramps. When no control is applied, the nominal speed limit for the first 1 km of the motorway stretch is 120 km/h and falls to 100 km/h for the following 1 km. Then, a speed limit of 80 km/h is applied at the downstream 4-lane part, through the merge area, and at the 3-lane part of the motorway. The capacity of the motorway upstream of the work zone area is sufficiently high to accommodate the investigated real demand scenario, while the downstream capacity is reduced due to the lane drop. Detectors have been placed at different positions along the simulated stretch for the collection of measurements that can be used for operation (as explained above) or evaluation purposes, as displayed in Fig. 2. The length of the acceleration area is set to 500 m as this is deemed sufficient for vehicles to accelerate from low speeds in the VSL application area to the critical speed through the bottleneck. A gantry displaying a constant VSL ("Capacity VSL") is located at the beginning of the acceleration area. The length of the application area is also set to 500 m and the corresponding gantry ("Main VSL") displaying the decision taken by the PI regulator (1) is placed at its upstream end. The most downstream detector station, close to the bottleneck, provides the real-time density estimates needed for the PI controller operation according to (1). Finally, the safety area is divided into three segments of 500 m each, and the corresponding VSL gantries are placed at the upstream end of each segment displaying speed limits based on the rules discussed earlier.

3.2 Microscopic Simulation Configuration

The described infrastructure was modelled using the microscopic simulator AIMSUN v.8.0 (TSS, 2014) while its microSDK tool was used to overwrite the simulator's default behavioral models. The default car-following model used to define the longitudinal movement of vehicles in AIMSUN, is based on the model developed by Gipps (1981). This model, however, cannot always reproduce capacity drop phenomena in critical regimes (Wang et al., 2005), and, for this reason, it was replaced with the Intelligent Driver Model (IDM) car-following model (Treiber et al., 2000) as applied in (Ntousakis et al., 2015). The IDM can reflect significant aspects of the traffic flow dynamics and shows crash-free collective dynamics (Kesting et al., 2010). The default lane-changing model employed in AIMSUN is the Gipps lane-changing model (Gipps, 1986). The main limitation of this model is that it cannot capture realistically the merging behavior in a critical flow regime (Chevallier and Leclercq, 2009), and therefore it is complemented at critical merging locations with some heuristic rules (Roncoli et al., 2014). This rule-based lane-change modelling approach is applied here to the lane-drop region where the default model may result in standing vehicles and unreasonably long queues; while in the rest of the motorway, the Gipps lane-changing model is used unchanged.

3.3 Model Calibration

Besides the assigned behavioral models, the dynamic traffic scenario needs to be defined for the microscopic simulation model. The real data retrieved from the field measurements, consist of speed and flow measurements collected in several days, whereby a distinction between car and truck flows and speeds is made by the measurement devices. The dataset collected on 28.09.2015 is selected for model calibration,

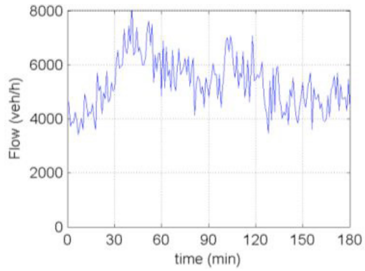

Fig. 3. Real demand profile at the entrance of the motorway stretch.

while datasets from other days are used in order to test the validity of the calibrated model. The duration of the simulation is 3 hours (from 5:45 am to 8:45 am), which cover the formation and dissipation of mainstream congestion upstream of the work zone area, and the real demand scenario is depicted in Fig. 3. At the beginning, the average demand at the motorway entrance starts at low values around 4000 veh/h. The demand increases gradually within the first 40 min, until it reaches a peak demand of almost 8000 veh/h. Trucks have been included in the demand according to the real data. Fig. 4 presents the contour plot produced using real speed measurements. It can be observed that congestion is created at the lane-drop area, which spills back and covers almost the whole upstream motorway stretch.

The reliability of the microscopic simulation is ensured with the calibration of the model parameters so as to achieve simulation results close to reality. To this end, once the case study network described above is cautiously modeled and the dynamic demand scenario is created in the microscopic traffic simulator, a sensitivity analysis was conducted to identify the model parameters that have the biggest impact on the simulation output. The most significant parameters of AIMSUN to be tuned were found to be maximum acceleration, comfortable deceleration, time headway, desired speed, maximum give-way time, and minimum distance.

The calibration of those model parameters is a time consuming and challenging task, since they have to be calibrated simultaneously, taking into account the correlation between the selected parameters. Due to space restrictions, more details on the calibration procedure can be found in (Heinrich et al., 2016). Fig. 5 presents the contour plot produced using the simulated speed outcome after calibration. It can be observed that congestion is created at the same place (merge area) and at the same time compared to the real data. The congestion spills back, covering the upstream motorway stretch, and lasts for the same time period as in reality.

The calibrated model has been further validated in order to confirm that it can replicate real traffic phenomena under other conditions as well. To this end, different demand profiles, based on real data collected from different days, were employed, and it was concluded that the microscopic simulation can indeed approach reality under other conditions as well, see (Heinrich et al., 2016) for details.

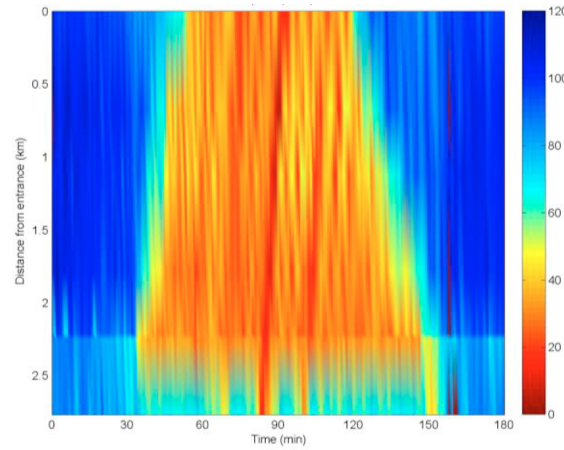

Fig. 4. Real speed (km/h) contour plot for the motorway stretch.

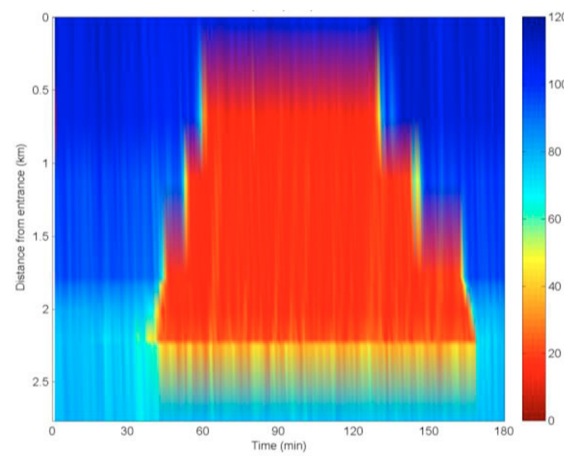

Fig. 5. Simulated speed (km/h) contour plot for the motorway stretch.

3.4 Application of the Control Framework

For the application of the control framework, the feedback regulator (1) is activated every control period T (=1 min) and receives the real-time estimates of density at the bottleneck area to calculate the "Main VSL" to be displayed in the next control period k, so as to maintain the density around its critical value. The VSL delivered by the PI regulator is rounded to the closest multiple of 10 km/h to obtain the corresponding posted VSL. Furthermore, the difference between two consecutively posted VSL at the same gantry is limited to 10 km/h, and the difference between two VSL posted at consecutive gantries (safety area) at the same control period is limited to 10 km/h. Also, a posted VSL value is not allowed to be higher than the speed measurement at the same point, rounded to the next multiple of 10 km/h. Finally, a constant speed limit of 80 km/h is applied at the start of the acceleration area.

The specification of appropriate regulator parameter values was conducted manually, via a trial-and-error procedure. Specifically, various sets of values were tested through a series of simulation runs. The employed regulator is not very sensitive to the distance between the measurement point and the control device; in fact, the parameter values resulted from this investigation were found to work equally well for different positions of the VSL gantries as well.

The implementation of the control strategy was done via the AIMSUN API (Application Programming Interface), which allows the user to emulate a real-time control environment. Specifically, the simulator delivers measurements at every control period T; based on these measurements, the control software calculates the corresponding VSL settings for all gantries and returns them to the microscopic simulator for application. Since the AIMSUN simulator model is stochastic, different replications with different random seeds may produce different results. Apart from the replication used for calibration purposes (ID 378), nine more replications have been run in order to produce statistically meaningful results.

It should be emphasized that the proposed regulator does not use any traffic flow model; it merely reacts to real-time measurements, both in the present simulations and in potential field applications. Thus, given the known inherent robustness of feedback regulators, a similar kind of control behavior (and resulting improvements), as obtained here, may be expected in practice.

4. SIMULATION RESULTS

4.1 No-Control Case

In the no-control case, arriving vehicles enter the merge area and exit without any serious problem, as long as the arriving demand is sufficiently low. When the demand increases (peak period) beyond the work zone capacity, vehicle merging conflicts are observed that lead to vehicle decelerations and formation of congestion. Congestion spills back, and the resulting Average Vehicle Delay (AVD) for the calibrated replication (ID 378) is 53.8 s/veh/km, while the Average Density (AD) is 32.4 veh/km and the Average Harmonic Speed (AHS) is 39.6 km/h. The trajectories in Fig. 6 display the flow, occupancy, density and speed measurements at the bottleneck area. The corresponding fundamental diagram is displayed as well. Fig. 4, discussed already above, displays the speed contour plot for the whole motorway stretch.

Occupancy/density at the merge area is gradually increasing within the first 40 min (as a consequence of the increasing demand), while the merge area outflow is seen to follow the increase of arriving demand, reaching for a small period the value of 6000 veh/h. At $t = 42$ min, the merge area occupancy/density increases steeply due to serious merging conflicts that lead to a speed breakdown, and this congested traffic situation becomes stationary until $t = 170$ min. The outflow during this time period is reduced to around 5000 veh/h on average due to the merge area congestion (capacity drop). After $t = 170$ min, the merge area occupancy/density is seen to drop, and the outflow reduces to lower values due to the decreased demand. Speed measurements at the merge area indicate that, during the peak period queuing, there is a serious speed drop down to around 25 km/h on average, while in the rest of the simulation horizon the average vehicle speed is around 75 km/h on average.

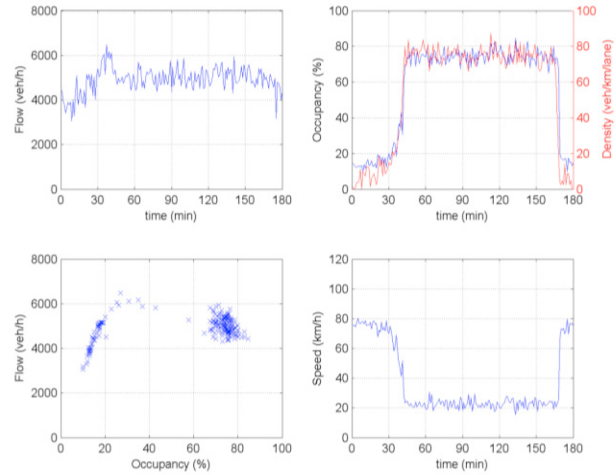

Fig. 6. Flow, occupancy, density and speed measurements at the bottleneck area for the no-control case (ID 378).

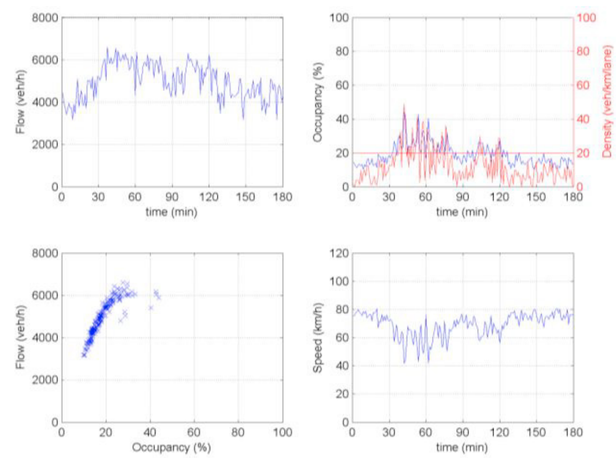

Fig. 7. Flow, occupancy, density and speed measurements at the bottleneck area for the VSL-control case (ID 378).

4.2 VSL-Control Case

For the VSL-control case, the critical density utilized by the PI-regulator as a set-point is 20 veh/km/lane as this was the density for which capacity flow is achieved in the no-control case. The maximum and minimum VSL values utilized for truncation of the value calculated by the regulator are set to 100 km/h and 20 km/h, respectively. Although 20 km/h is a very low speed limit, this bound was chosen in order to provide maximum flexibility, and hence maximum efficiency, to the regulator. Note that such low values are anyhow encountered for long time periods in the no-control case due to congestion. In addition, the provisional and exceptional character of a work zone environment may allow for the display of low VSL over short periods of time for the sake of increased safety and efficiency.

Fig. 7 displays flow, occupancy, density and speed measurements, as well as the corresponding fundamental diagram at the bottleneck area, while Fig. 8 displays the speed contour plot for the whole motorway stretch.

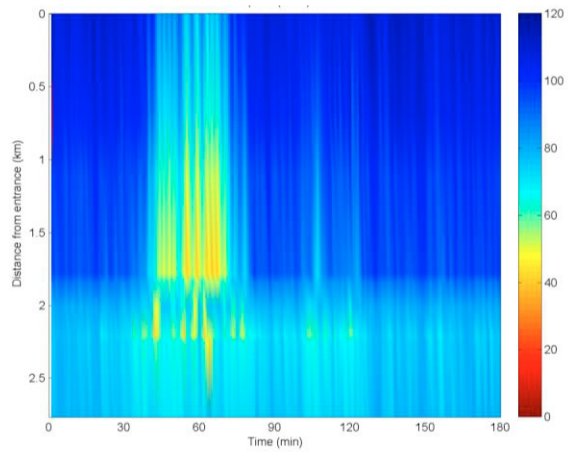

Fig. 8. Speed contour plot for the VSL-control case (Replication ID 378).

Table 1. VSL-control case – Decrease of performance indexes compared to the no-control case per replication.

ID	AVD	AD	AHS	TDT	TTT	Stops
378	84.6%	53.1%	-100.3%	-1.1%	53.1%	91.0%
477	74.0%	46.1%	-74.4%	-0.3%	46.2%	77.9%
478	83.5%	51.3%	-92.5%	-0.6%	51.3%	93.9%
479	67.3%	40.2%	-57.6%	0.0%	40.3%	72.2%
480	77.5%	49.8%	-88.2%	-1.3%	49.8%	85.0%
481	77.1%	49.5%	-87.0%	-1.1%	49.5%	80.9%
482	72.7%	45.0%	-71.2%	-0.2%	45.1%	77.3%
483	79.2%	52.1%	-96.4%	-1.6%	51.9%	83.4%
484	79.3%	49.6%	-85.7%	-0.3%	49.6%	87.9%
485	85.4%	53.5%	-101.5%	-0.7%	53.6%	93.5%
Mean Value	78.3%	49.2%	-85.0%	-0.7%	49.2%	84.5%

The maximum VSL value is ordered by the regulator for as long as density remains well undercritical. As the demand increases, density increases as well, and, as it is approaching its critical value, the controller starts its actual operation aiming to maintain density around its critical value. This is actually achieved without ever reaching the VSL minimum value. Capacity flow (about 6200 veh/h) is achieved for long periods without any capacity drop at the bottleneck area. At this time, a queue is formed upstream of the VSL gantry (since the arriving demand is higher than the work zone capacity) which propagates backwards. However, the higher outflow of the system leads quickly to the resolution of the congestion, already at $t = 70$ min. The resulting AVD for the same replication (ID 378) is 8.3 s/veh/km which is a 84.6% decrease; AD is 15.2 veh/km which is a 53.1% decrease; while the AHS is 79.2 km/h which is a 100.3% increase compared to the no-control case.

Table 1 presents the average improvement, compared to the no-control case, of various performance indexes for 10 replications. These performance indexes include AVD, AD, AHS, the Total Distance Travelled (TDT), the Total Travel Time (TTT) and the Number of Stops. Remarkable improvements can be observed for all performance indexes and for all replications simulated. It must be noted at this point that the performance indexes have been calculated also separately for cars and trucks, but they are not reported here because on average the improvements achieved are close to the ones presented for all vehicles.

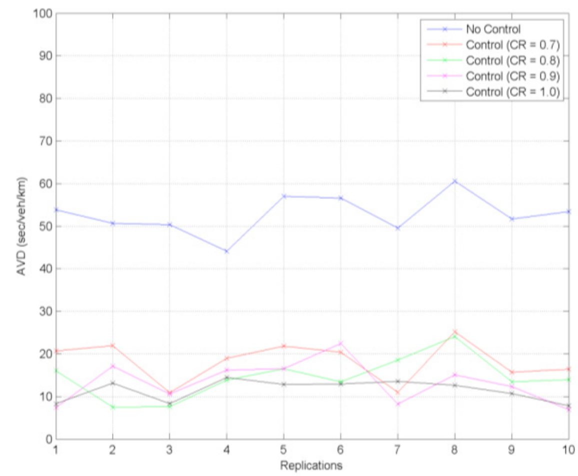

Fig. 9. Average Vehicle Delay (AVD) per Replication for the no-control case and control cases with different compliance rate (CR).

4.3 Compliance Rate

Investigations were carried out to determine the influence of the compliance rate (CR) on the results achieved in the control case. A CR value of 1.0 was used for the results so far. Simulation studies were also performed for different CRs. Fig. 9 presents a graphical comparison for AVD, while the results for the other performance indexes are analogous. As expected, a decrease of the compliance rate leads only to moderate deterioration of the performance. This can be attributed to two factors:

- The feedback character of the control system, which, if the drivers do not adequately comply, continues with adequate VSL displays as long as necessary to achieve the required effect in the real-time measurements.
- The good compliance of some drivers can, given the limited chances of lane changing, prevent less disciplined drivers from achieving high speeds, thus increasing the factual compliance rate of the whole vehicle population.

4.4 Critical density set point

The positive control performance achieved is primarily the result of the flow maximization at the bottleneck area, which is achieved indirectly, by regulating the traffic density at its critical value. The set-point used for the feedback controller is 20 veh/km/lane. Since the respective critical value is previously unknown and possibly subject to some stochastic changes, it is interesting to investigate the influence of the employed critical density value on the control results.

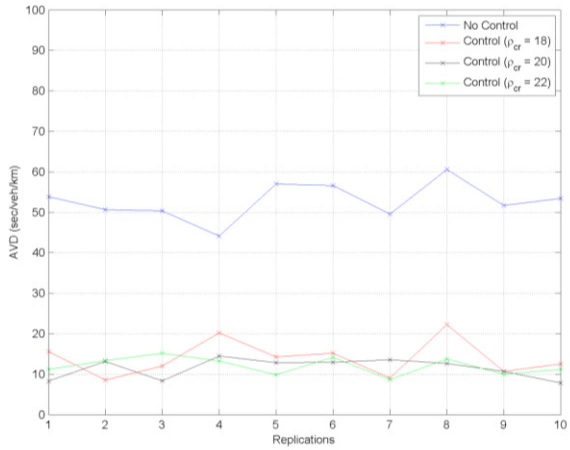

Fig. 10. Average Vehicle Delay (AVD) per Replication for the no-control case and control cases with different critical occupancy as a set point.

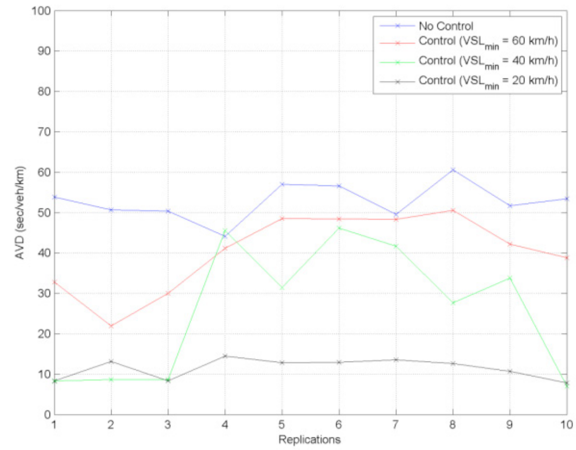

Fig. 11. Average Vehicle Delay (AVD) per Replication for the no-control case and control cases with different minimum VSL values.

For this purpose, the simulation tests were carried out again with different set-points. The target values now under investigation are 18 and 22 veh/km/lane, and the corresponding results of the 10 replications are summarized in Fig. 10 on the basis of the performance index AVD. The results indicate a low sensitivity of the control quality as a function of the set-point used, as long as this is selected within a suitable range of values. As a result, the expected calibration effort for establishing a suitable set-point is expected to be low in practice.

4.5 Minimum VSL Value

As already mentioned, the major part of the control efficiency results from the possibility of keeping the bottleneck largely free of congestion by the action of the feedback controller and, moreover, to operate it at its capacity. The actuator for this operation is the "Main VSL" gantry, which was allowed to display VSL values down to the permissible minimum value of 20 km/h. Although this minimum value was not reached at any time during the replication with ID 378, this might be necessary for short periods of time in other cases. Although, even if it sounds paradoxical, this low value can drastically shorten travel times, the question of the acceptance of such low VSL by the drivers or the highway operators is certainly justified. In order to obtain further decision-making grounds for the relevant discussion, the simulation examinations were carried out again, with different permissible minimum values for the main VSL gantry.

The minimum values are now set to 40 km/h and 60 km/h, and the corresponding results of the 10 replications are summarized in Fig. 11 on the basis of the performance index AVD. It can be seen that the result of this critical sensitivity analysis is different than in the two previous analyses since the control efficiency actually depends strongly on the permissible VSL minimum value. At a minimum of 40 km/h, two classes of replications are observed. The first class concerns replications 1, 2, 3 and 10, where the control efficiency, compared with the original case of a minimum value of 20 km/h, does not suffer any damage. The second class concerns the remaining six replications in which the control efficiency is significantly better than in the case of no control, but is significantly reduced compared to the original case of a minimum value of 20 km/h. At the minimum value of 60 km/h, two classes of replications are also observed, with the first class now containing replications 1, 2 and 3, with control efficiency, as compared to the original case of a minimum value of 20 km/h, presenting a small deterioration. The second class includes the remaining seven replications, where the control efficiency is better than in the case of no control, but is significantly reduced compared to the original case of a minimum value of 20 km/h.

A more detailed discussion of these results may be found in (Heinrich et al., 2016), along with suggestions on how to deal with the issue of the minimum admissible VSL value, and corresponding investigations are currently on-going.

5. CONCLUSION

A novel real-time merging traffic control approach aiming at throughput maximization at highway work zones using VSL was presented. A PI feedback regulator was employed for control which is simpler and potentially more robust compared to heuristic or optimal control procedures. Practical VSL implementation aspects were taken into account. The proposed concept was tested using a validated microscopic traffic flow model for a real motorway work zone in Germany. Significant improvements were observed for all performance indexes considered and for all replications simulated. Investigations were carried out for different compliance rates, different set points utilized by the feedback regulator, as well as for different values of the lower bound applied on the VSL. The proposed approach is deemed suitable for field implementation.

ACKNOWLEDGEMENTS

This paper is based on parts of the research project carried out at the request of the Federal Ministry of Transport and Digital Infrastructure, Germany, represented by the Federal

Highway Research Institute, under the research project No. 03.0533/2015/FRB. The data was provided by the Traffic Management Center Straßen.NRW located in Leverkusen, Germany. The authors are solely responsible for the contents of the paper.

REFERENCES

FHWA. *Developing and Implementing Transportation Management Plans for Work Zones*. Report of the Federal Highway Administration, U.S. Department of Transportation, 2005.

Papageorgiou, M., Papamichail, I., Spiliopoulou, A.D. and Lentzakis, A.F. (2008). Real-time merging traffic control with applications to toll plaza and work zone management. *Transp. Res. Part C*, 16, 535–553.

Yuan, K., Knoop, V.L. and Hoogendoorn, S.P. (2015). Capacity drop: relation between the speed in congestion and the queue discharge rate. *Transp. Res. Record*, 2491, 72–80.

Yuan, K. (2016). Capacity Drop on Freeways: Traffic Dynamics, Theory and Modeling. PhD Thesis, Delft University of Technology.

Lin, P.W., Kang, K.P. and Chang, G.L. (2004). Exploring the effectiveness of variable speed limit controls on highway work-zone operations. *Journal of Intell. Transp. Systems*, 8, 155–168.

Kang, K.P, Chang, G.L. and Zou, N. (2004). Optimal dynamic speed-limit control for highway work zone operations. *Transp. Res. Record*, 1877, 77–84.

Wei, H. and Pavithranm M. (2006). Concept of dynamic merge metering approach for work zone traffic control. *11th IFAC Symposium on Control in Transportation Systems*, Delft, The Netherlands, 374–379.

Yang, N., Chang, G.L. and Kang, K.P. (2009). Simulation-based study on a lane-based signal system for merge control at freeway work zones. *Journal of Transp. Engineering*, 135, 9–17.

Kang, K.P., Chang, G.L. (2009). Lane-based dynamic merge control strategy based on optimal thresholds for highway work zone operations. *Journal of Transp. Engineering*, 135, 359–370.

Kwon, E., Brannan, D., Shouman, K., Isackson, C. and Arseneau, B. (2007). Developments and field evaluation of variable speed limit system for work zones. *Transportation Res. Record*, 2015, 12–18.

Carlson, R.C., Papamichail, I., Papageorgiou, M. and Messmer, A. (2010). Optimal mainstream traffic flow control involving variable speed limits and ramp metering. *Transp. Science*, 18, 193–210.

Lentzakis, A.F., Spiliopoulou, A.D., Papamichail, I. and Papageorgiou, M. (2008). Real-time work zone management for throughput maximization. *87th Transp. Res. Board Annual Meeting*, Washington, D.C.

Fudala, N.J. and Fontaine, M.D. (2010). Interaction between system design and operations of variable speed limit systems in work zones. *Transp. Res. Record*, 2269, 1–10.

Kang, K.P. and Chang, G.L. (2011). An integrated control algorithm of the advanced merge and speed limit strategies at highway work zones. *90th Annual Meeting of the Transp. Res. Board*, Washington, D.C.

Harb, R., Radwab, E., Abdel-Aty, M. and Su, X. (2011). Two simplified intelligent transportation system-based lane management strategies for short-term work zones. *Journal of Intell. Transp. Systems*, 15, 52–61.

Yang, X., Lu, Y. and Lin, Y. (2017). Optimal variable speed limit control system for freeway work zone operations. *Journal of Computing in Civil Engineering*, accepted.

Tympakianaki, A., Spiliopoulou, A., Kouvelas, A., Papamichail, I., Papageorgiou, M. and Wang, Y. (2014). Real-time merging traffic control for throughput maximization at motorway work zones. *Transp. Res. Part C*, 44, 242–252.

Vigos, G., Papageorgiou, M. and Wang, Y. (2008). Real-time estimation of vehicle-count within signalized links. *Transp. Res. Part C*, 16, 18–35.

Papageorgiou, M., Haj-Salem, H. and Blosseville, J.-M. (1991). ALINEA: A local feedback control law for on-ramp metering. *Transp. Res. Record*, 1320, 58–64.

Carlson R.C., Papamichail, I. and Papageorgiou, M. (2011). Local feedback-based mainstream traffic flow control on motorways using variable speed limits. *IEEE Tran. on Intell. Transp. Systems*, 12, 1261–1276.

Carlson R.C., Papamichail, I. and Papageorgiou, M. (2013). Comparison of local feedback controllers for the mainstream traffic flow on freeways using variable speed limits. *Journal of Intell. Transp. Systems*, 17, pp. 268–281.

TSS (2014). Aimsun 8 Dynamic Simulators Users' Manual.

Gipps, P. (1981). A behavioural car-following model for computer simulation. *Transp. Res. Part B*, 15, 105–111.

Wang, J., Liu, R. and Montgomery, F. (2005). Car-following model for motorway traffic *Transp. Res.* Record, 1934, 33–42.

Treiber, M., Hennecke, A. and Helbing, D. (2000). Congested traffic states in empirical observations and microscopic simulations. *Physical Review E*, 62, 1805–1824.

Ntousakis, I.A., Nikolos, I.K. and Papageorgiou, M. (2015). On microscopic modelling of adaptive cruise control systems. *Transp. Res. Procedia*, 6, 111–127.

Kesting, A., Treiber, M. and Helbing, D. (2010). Enhanced intelligent driver model to access the impact of driving strategies on traffic capacity. *Philosophical Trans. of the Royal Society A*, 368, 4585–4605.

Gipps, P. (1986). A model for the structure of lane-changing decisions. *Transp. Res. Part B*, 20, 403–414.

Chevallier, E. and Leclercq, L. (2009). Do microscopic merging models reproduce the observed priority sharing ratio in congestion? *Transp. Res. Part C*, 17, 328–336.

Roncoli, C., Papamichail, I. and Papageorgiou, M. (2014). Model predictive control for multilane motorways in presence of VACS. In *17th Int. IEEE Conf. on Intell. Transp. Systems*, 501–507.

Heinrich, T., Maier, F., Papageorgiou, M., Papamichail, I., Schober, C. and Stamatakis, I. (2016). Entwicklung einer Fahrstreifenreduktionsbeeinflussungsanlage für Baustellen auf BAB. Bundesanstalt für Straßenwesen, FE 03.0533/2015/FRB.